^{188}Re-$Z_{HER2:V2}$, a Promising Affibody-Based Targeting Agent Against HER2-Expressing Tumors: Preclinical Assessment

Mohamed Altai[1], Helena Wållberg[2], Hadis Honarvar[1], Joanna Strand[1], Anna Orlova[3], Zohreh Varasteh[3], Mattias Sandström[4,5], John Löfblom[2], Erik Larsson[6], Sven-Erik Strand[6], Mark Lubberink[4,5], Stefan Ståhl[2], and Vladimir Tolmachev[1]

[1]Division of Biomedical Radiation Sciences, Uppsala University, Uppsala, Sweden; [2]Division of Protein Technology, School of Biotechnology, KTH Royal Institute of Technology, Stockholm, Sweden; [3]Preclinical PET Platform, Department of Medicinal Chemistry, Uppsala University, Uppsala, Sweden; [4]Nuclear Medicine and PET, Uppsala University, Uppsala, Sweden; [5]Medical Physics, Uppsala University Hospital, Uppsala, Sweden; and [6]Medical Radiation Physics, Clinical Sciences, Lund University, Lund, Sweden

Affibody molecules are small (7 kDa) nonimmunoglobulin scaffold proteins with favorable tumor-targeting properties. Studies concerning the influence of chelators on biodistribution of ^{99m}Tc-labeled Affibody molecules demonstrated that the variant with a C-terminal glycyl-glycyl-glycyl-cysteine peptide–based chelator (designated $Z_{HER2:V2}$) has the best biodistribution profile in vivo and the lowest renal retention of radioactivity. The aim of this study was to evaluate ^{188}Re-$Z_{HER2:V2}$ as a potential candidate for radionuclide therapy of human epidermal growth factor receptor type 2 (HER2)–expressing tumors. **Methods:** $Z_{HER2:V2}$ was labeled with ^{188}Re using a gluconate-containing kit. Targeting of HER2-overexpressing SKOV-3 ovarian carcinoma xenografts in nude mice was studied for a dosimetry assessment. **Results:** Binding of ^{188}Re-$Z_{HER2:V2}$ to living SKOV-3 cells was demonstrated to be specific, with an affinity of 6.4 ± 0.4 pM. The biodistribution study showed a rapid blood clearance (1.4 ± 0.1 percentage injected activity per gram [%ID/g] at 1 h after injection). The tumor uptake was 14 ± 2, 12 ± 2, 5 ± 2, and 1.8 ± 0.5 %IA/g at 1, 4, 24, and 48 h after injection, respectively. The in vivo targeting of HER2-expressing xenografts was specific. Already at 4 h after injection, tumor uptake exceeded kidney uptake (2.1 ± 0.2 %IA/g). Scintillation-camera imaging showed that tumor xenografts were the only sites with prominent accumulation of radioactivity at 4 h after injection. Based on the biokinetics, a dosimetry evaluation for humans suggests that ^{188}Re-$Z_{HER2:V2}$ would provide an absorbed dose to tumor of 79 Gy without exceeding absorbed doses of 23 Gy to kidneys and 2 Gy to bone marrow. This indicates that future human radiotherapy studies may be feasible. **Conclusion:** ^{188}Re-$Z_{HER2:V2}$ can deliver high absorbed doses to tumors without exceeding kidney and bone marrow toxicity limits.

Key Words: HER2; Affibody molecule; ^{188}Re; dosimetry

J Nucl Med 2014; 55:1842–1848
DOI: 10.2967/jnumed.114.140194

Overexpression of the human epidermal growth factor receptor type 2 (HER2) is associated with malignant transformation of cells and provides a growth advantage for tumors. Treatment of HER2-expressing disseminated tumors with the anti-HER2 monoclonal antibody trastuzumab improves survival in patients with metastatic breast (*1*) and gastric cancer (*2*). However, many tumors have a primary trastuzumab resistance or develop resistance during therapy despite preserved HER2 expression (*2*). Conjugation of cytotoxic payloads (e.g., drugs or radionuclides) to tumor-targeting antibodies may enhance their antitumor effects and hence improve the response duration and overall response rate (*3,4*). β-emitting radionuclides are considered a promising form of cytotoxic payload, because of the cross-fire effect. The use of full-length antibodies for radionuclide therapy, however, is associated with several issues. The major obstacles are insufficient penetration in the tumor tissue, limiting the absorbed dose to tumors and slow clearance from the body, causing second-organ (mainly bone marrow) toxicity (*5*). The use of smaller targeting agents, such as antibody fragments, would provide more efficient extravasation, better tumor penetration, and more rapid clearance of an unbound tracer (*6,7*).

A promising approach for development of high-affinity small tumor-targeting agents is the use of engineered scaffold proteins (*8*). Affibody (Affibody AB) molecules are the most studied class of scaffold proteins for in vivo radionuclide targeting. These high-affinity ligands are based on a 58-amino-acid (7 kDa) triple α-helical scaffold derived from domain B of staphylococcal protein A (*9*). An Affibody with picomolar affinity (22 pM) to the extracellular domain of HER2 has been selected earlier (*10*). Affibody molecules labeled with different radionuclides have demonstrated efficient tumor targeting and high-contrast imaging of HER2-expressing tumors (*11*). Two clinical studies have demonstrated that Affibody molecules are nontoxic and nonimmunogenic in humans (*12,13*). However, Affibody molecules undergo renal excretion followed by substantial renal reabsorption (*14*). The use of residualizing labels has therefore resulted in a high retention of radionuclides in kidneys, with a radioactivity concentration exceeding severalfold the radioactivity concentration in tumors. This would make the use of most radiometals (e.g., ^{177}Lu or ^{90}Y) unsuitable for radionuclide therapy (*11*). An important feature of the

Received Mar. 13, 2014; revision accepted Aug. 6, 2014.
For correspondence or reprints contact: Vladimir Tolmachev, Biomedical Radiation Sciences, Uppsala University, Se-75185, Uppsala, Sweden.
E-mail: vladimir.tolmachev@bms.uu.se
Published online Oct. 2, 2014.

HER2-targeting Affibody molecules is their slow internalization by HER2-expressing cells (*15*), enabling the use of nonresidualizing labels without appreciable reduction of tumor retention. In contrast, rapid internalization of the Affibody in proximal tubuli results in rapid clearance of nonresidualizing labels from kidneys (*11,16*).

Earlier, we evaluated how the composition of peptide-based N_3S chelators can influence the targeting and biodistribution properties of ^{99m}Tc-labeled Affibody molecules. Mercaptoacetyl-containing chelators on the N terminus (*17–20*) and cysteine-containing chelators on the C terminus (*21–23*) were evaluated. We showed that biodistribution of Affibody molecules can be altered by varying the amino acid composition of such chelators. Importantly, residualizing properties of the ^{99m}Tc label can be modulated in a wide range. For example, a ^{99m}Tc-labeled variant having a -GGGC peptide chelator at the C terminus (designated ^{99m}Tc-$Z_{HER2:V2}$) demonstrated tumor uptake exceeding renal uptake appreciably because of weak residualizing properties (*22*).

Rhenium is a chemical analog to technetium. The β-emitting rhenium isotope ^{188}Re (half-life, 17.0 h; maximum β energy, 2.1 MeV) has a potential for therapeutic applications. Production via a generator with the long-lived mother nuclide ^{188}W (half-life, 70 d) makes this radionuclide readily available with high specific radioactivity. A low-abundance (15%) low-energy (155 keV) γ emission enables imaging of the biodistribution of ^{188}Re-labeled therapeutic agents in patients for patient-specific dosimetry. We expected that substitution of ^{99m}Tc for ^{188}Re in Affibody molecules might provide a conjugate with a high tumor uptake and low renal retention. However, the chemical properties of rhenium and technetium are similar but not identical, and biodistribution of ^{99m}Tc- and ^{188}Re-labeled peptides can be different (*24,25*). Therefore, an evaluation of ^{188}Re-labeled $Z_{HER2:V2}$ was necessary.

The goal of the current study was to evaluate the tumor-targeting properties and biokinetics of ^{188}Re-$Z_{HER2:V2}$ in mice bearing HER2-expressing xenografts and, based on dosimetry evaluation, determine whether ^{188}Re-$Z_{HER2:V2}$ might be a candidate for treatment of HER2-expressing tumors without severe second-organ toxicity.

MATERIALS AND METHODS

^{188}Re was obtained as perrhenate by elution of a ^{188}W/^{188}Re generator (29.6 GBq) with 0.9% sodium chloride (Polatom). Affibody molecule $Z_{HER2:V2}$ was produced and purified as described previously (*26*). All chemicals were purchased from Sigma-Aldrich. The HER2-expressing ovarian cancer cell line SKOV-3, 1.6×10^6 HER2 receptors per cell (ATCC), was used in cell studies. Cells were cultured in RPMI medium supplemented with 10% fetal calf serum, 2 mM L-glutamine, and PEST (penicillin, 100 IU/mL, and streptomycin, 100 μg/mL).

Labeling and Stability

$Z_{HER2:V2}$ Affibody molecules were site-specifically labeled with ^{188}Re using freeze-dried labeling kits containing 5 mg of sodium α-D-gluconate, 100 μg of disodium ethylenediaminetetraacetic acid, and 1 mg of tin(II) chloride dihydrate. After reconstitution, labeling was performed at pH 4.2 and 90°C for 1 h. Ascorbic acid and bovine serum albumin were introduced as antioxidants, as described in the supplemental materials (available at http://jnm.snmjournals.org).

To evaluate serum stability, freshly labeled ^{188}Re-$Z_{HER2:V2}$ (10 μL) was diluted in a serum sample (200 μL) to a concentration similar to the concentration in blood at the moment of injection and was incubated for 1 h at 37°C. The mixture was analyzed using radio–sodium dodecylsulfate polyacrylamide gel electrophoresis. A sample of perrhenate was used as a reference. The analysis was performed in duplicate.

In Vitro Evaluation

The specificity of binding and cellular processing of ^{188}Re-$Z_{HER2:V2}$ by SKOV-3 cells were evaluated as described previously (*15*). The affinity of ^{188}Re-$Z_{HER2:V2}$ binding to SKOV-3 was measured at 4°C using LigandTracer (Ridgeview Instruments AB) with 2 concentrations: 49 pM and 98 pM (details of the in vitro experiments are provided in the supplemental materials).

In Vivo Studies

The animal experiments were planned and performed in accordance with national legislation on laboratory animals' protection. The animal study was approved by the local Ethics Committee for Animal Research in Uppsala.

SKOV-3 cells (10^7 cells per mouse) were implanted on the right hind leg of female NMRI (Naval Medical Research Institute) *nu/nu* mice. The average animal weight was 27 ± 2 g, and the average tumor weight was 0.8 ± 0.2 g at the start of the experiment. Six groups of mice (4 per group) were injected intravenously with ^{188}Re-$Z_{HER2:V2}$ in 100 μL of phosphate-buffered saline. The injected radioactivity was 53 kBq/mouse for 6 groups. The injected protein dose was adjusted to 1 μg/mouse by adding nonlabeled $Z_{HER2:V2}$. The animals were euthanized at 20 min, 1 h, 4 h, 8 h, and 24 h after injection. One group was injected with 140 kBq/mouse and euthanized at 48 h after injection. For specificity control, 1 group of 3 mice was preinjected with 500 μg of $Z_{HER2:342}$ 45 min before injection of ^{188}Re-$Z_{HER2:V2}$ and euthanized at 4 h after injection. Organs and tissue samples (Table 1), gastrointestinal tract, and the remaining carcass were collected and weighed, and their radioactivity was measured in a NaI(Tl) well counter (PerkinElmer). Biodistribution data were corrected for decay and self-attenuation in samples, and organ uptake values were calculated as percentage injected activity per gram (%IA/g), except for the intestinal content, thyroid, and carcass, which were calculated as %IA per whole sample.

In vivo imaging was performed to visually confirm the biodistribution data. Three SKOV-3–bearing mice were injected with 0.7 MBq (8 μg) of ^{188}Re-$Z_{HER2:V2}$. Two mice were injected 4 h before the imaging experiment and 1 mouse 1 h before. Immediately before imaging, the mice were sacrificed by cervical dislocation and the bladders were excised. The imaging was performed using an Infinia scintillation camera (GE Healthcare) equipped with a high-energy general-purpose collimator. Static images (30 min) were obtained with a zoom factor of 2 in a 256 × 256 matrix.

Dosimetry

Animal Dosimetry. To evaluate the feasibility of experimental therapy in mice, absorbed doses to tumors and normal tissues were calculated using the anatomically realistic murine Moby phantom developed by Larsson et al. (*27,28*) based on the biokinetics results. Absorbed doses per injected activity (Gy/MBq) for ^{188}Re-$Z_{HER2:V2}$ were calculated for 3 tumor locations: the right hind leg, left hind leg, and left flank.

Human Dosimetry. For dosimetry estimations in humans, uptake was extrapolated from animal data according to the percentage kg/g method (*29*).

$$(\%\mathrm{IA/organ})_{\mathrm{human}} = \left[(\%\mathrm{IA/g})_{\mathrm{animal}} \times \left(\mathrm{kg_{TBweight}}\right)_{\mathrm{animal}} \times \left(\mathrm{g_{organ}}/\left(\mathrm{kg_{TBweight}}\right)_{\mathrm{human}}\right]\right.,$$

where TB is total body. Organ time–activity curves were calculated using the organ weights of the 58-kg reference adult female (ICRP publication 23). Residence times were calculated as the area under the curve of biexponential fits to the animal organ time–activity curves. Remainder-of-body residence time was based on radioactivity in the carcass. Red marrow activity concentrations were conservatively

TABLE 1
Biodistribution of ^{188}Re-$Z_{HER2:V2}$ in NMRI *nu/nu* Mice Bearing HER2-Expressing SKOV-3 Xenografts

Organ	Uptake					
	20 min	1 h	4 h	8 h	24 h	48 h
Blood	3.0 ± 0.3	1.4 ± 0.1	0.3 ± 0.1	0.05 ± 0.02	0.02 ± 0.01	0.006 ± 0.003
Heart	1.4 ± 0.3	0.6 ± 0.1	0.11 ± 0.02	0.05 ± 0.01	0.02 ± 0.01	NM
Lung	3.4 ± 0.2	1.7 ± 0.2	0.28 ± 0.05	0.08 ± 0.03	0.03 ± 0.01	NM
Salivary gland	1.6 ± 0.5	1.1 ± 0.3	0.2 ± 0.1	0.06 ± 0.03	0.02 ± 0.01	NM
Thyroid*	0.07 ± 0.02	0.04 ± 0.02	0.01 ± 0.001	0.01 ± 0.004	0.002 ± 0.001	NM
Liver	3.4 ± 0.3	2.2 ± 0.2	0.51 ± 0.09	0.26 ± 0.06	0.12 ± 0.03	0.06 ± 0.016
Spleen	1.5 ± 0.2	0.87 ± 0.06	0.16 ± 0.02	0.08 ± 0.01	0.03 ± 0.01	NM
Pancreas	0.8 ± 0.2	0.4 ± 0.1	0.08 ± 0.03	0.030 ± 0.003	0.01 ± 0.01	NM
Stomach	2.0 ± 0.08	1.3 ± 0.23	0.3 ± 0.1	0.08 ± 0.01	0.08 ± 0.07	NM
Small intestine	1.4 ± 0.1	0.9 ± 0.2	0.16 ± 0.08	0.08 ± 0.07	0.04 ± 0.03	NM
Large intestine	1.9 ± 0.08	1.2 ± 0.6	0.19 ± 0.05	0.3 ± 0.3	0.04 ± 0.01	0.02 ± 0.004
Kidney	47 ± 2	18 ± 3	2.1 ± 0.2	1.0 ± 0.2	0.51 ± 0.08	0.30 ± 0.12
Tumor	8.7 ± 0.9	14 ± 2	12 ± 2	8.0 ± 0.6	5 ± 2	1.8 ± 0.5
Skin	2.4 ± 0.4	1.4 ± 0.1	0.6 ± 0.5	0.10 ± 0.02	0.04 ± 0.02	0.02 ± 0.005
Muscle	0.6 ± 0.1	0.28 ± 0.03	0.06 ± 0.03	0.02 ± 0.01	0.02 ± 0.01	NM
Bone	1.0 ± 0.1	0.6 ± 0.1	0.12 ± 0.01	0.05 ± 0.02	0.04 ± 0.02	NM
Brain	0.08 ± 0.02	0.05 ± 0.01	0.020 ± 0.003	0.01 ± 0.001	0.01 ± 0.002	NM
Carcass*	23 ± 2	14 ± 4	2 ± 1	1.1 ± 0.9	0.35 ± 0.09	0.19 ± 0.04

*Data for thyroid and carcass are presented as %IA per whole sample.
NM = not measurable, below detection limit.
Uptake is expressed as %IA/g and presented as average value from 4 animals ± SD. Data are corrected for decay and self-attenuation in samples.

assumed to equal whole-blood concentrations. Absorbed doses were estimated using OLINDA/EXM 1.0. For calculation of absorbed dose to the intestines, either the ICRP 30 gastrointestinal model was applied, using a fraction of 0.35 %IA (the measured value at 1 h after injection) entering the small intestine, or residence times calculated as above for small intestine and large intestine were used.

In tumor, standardized uptake value was assumed to be identical in humans and rodents, and tumor-absorbed doses were calculated assuming deposition of all β energy within the tumor, neglecting any self- or cross-dose from γ radiation. Dependence of absorbed dose on tumor volume was assessed using the OLINDA/EXM 1.0 sphere model.

RESULTS

Labeling and Stability

The labeling method provided high yield (95.8% ± 1%), with radiocolloid content below 1%. Purification using disposable NAP-5 columns (GE Healthcare) provided radiochemical purity over 99%. Up-scaling experiments demonstrated that specific activity of 17.5 MBq/μg (116 GBq/μmol) can be obtained. ^{188}Re-$Z_{HER2:V2}$ was stable in the formulation containing 6 mM ascorbic acid in phosphate-buffered saline with 2% bovine serum albumin (radiochemical purity of 99% ± 1% during 4 h). In the absence of bovine serum albumin, radiochemical purity was 94% ± 2% after 4 h.

Sodium dodecylsulfate polyacrylamide gel electrophoresis was performed after incubation in murine blood plasma at 37°C for 60 min. The main peak corresponded to the monomeric Affibody molecule. No peaks indicating aggregation of Affibody molecules or transchelation of the radionuclide to blood proteins were observed. The only other radioactivity peak had a path length equal to the path length of ^{188}Re-perrhenate. This peak contained less than 2% of the total activity at the end of the stability test (Supplemental Fig. 1).

In Vitro Evaluation

The in vitro specificity experiment showed that binding of ^{188}Re-$Z_{HER2:V2}$ to SKOV-3 ovarian carcinoma cells can be reduced from 52% ± 1% to 0.84% ± 0.05% of added activity ($P < 0.0001$) by presaturation of HER2 with nonlabeled Affibody molecule. This indicates that the binding of ^{188}Re-$Z_{HER2:V2}$ was specific. The affinity of ^{188}Re-$Z_{HER2:V2}$ binding to SKOV3 cells at 4°C was 6.4 ± 0.4 pM (Supplemental Fig. 2).

The cellular retention profile (Fig. 1) showed a rapid drop in activity during the first hour followed by a slow decline with a biologic half-life of 19.6 h. The total cellular retention of the radioactivity was 34.6% ± 1.3% after 24 h of incubation at 37°C. The internalized radioactivity of ^{188}Re-$Z_{HER2:V2}$ was relatively low, less than 4% of total radioactivity after 24 h.

In Vivo Studies

The results of the in vivo specificity test (Fig. 2) showed that presaturation of HER2 in xenografts with a parental $Z_{HER2:342}$ decreased tumor uptake of ^{188}Re-$Z_{HER2:V2}$ 4.5-fold ($P < 0.005$). This demonstrates a saturable character of the tumor accumulation and suggests its HER2 specificity. A small but statistically significant

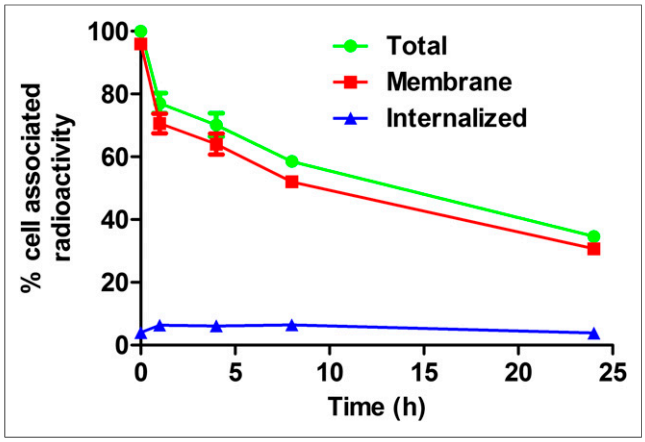

FIGURE 1. Cell-associated radioactivity as function of time after interrupted incubation of SKOV-3 cells with ^{188}Re-$Z_{HER2:V2}$. Data are presented as average value from 3 cell dishes ± SD. Error bars might not be seen because they are smaller than point symbols.

decrease in uptake in liver and an increase in kidneys was also detected in this experiment.

Biodistribution of ^{188}Re-$Z_{HER2:V2}$ in tumor-bearing mice (Table 1) was characterized by rapid clearance of radioactivity from all organs and tissues. Low radioactivity in the content of the gastrointestinal tract (<2% of injected activity; data not shown) suggested that the hepatobiliary pathway played a minor role in the excretion of ^{188}Re-$Z_{HER2:V2}$ or its radiometabolites. Low radioactivity uptake in organs accumulating free perrhenate, that is, salivary gland, thyroid, and stomach, suggests high stability of ^{188}Re-$Z_{HER2:V2}$ to reoxidation in vivo. The kidneys demonstrated high initial uptake, which decreased rapidly. At 1 h after injection, renal uptake was approximately equal to tumor uptake, and at 4 h after injection, tumor uptake was 5-fold higher.

Uptake was prominent in tumor as early as 20 min after injection and was higher than in any normal organ except the kidneys. Tumor uptake maximized at 1 h after injection (14 ± 2 %IA/g), followed by a decrease with a half-life of 15 h.

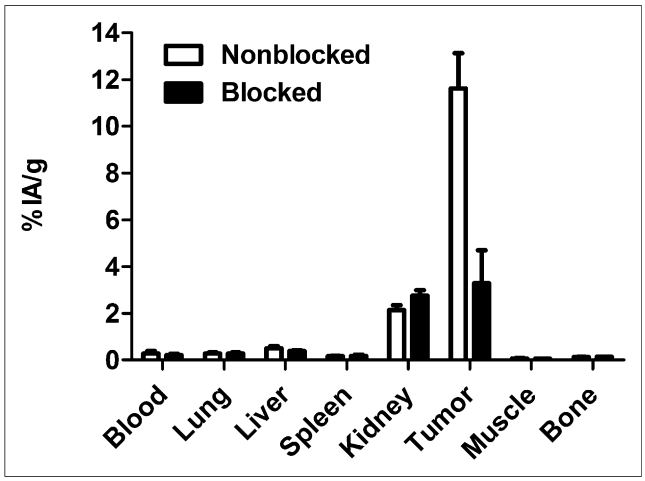

FIGURE 2. In vivo binding specificity of ^{188}Re-$Z_{HER2:V2}$ in mice bearing ovarian cancer SKOV-3 xenografts at 4 h after injection. Blocked group was subcutaneously preinjected with excess amount of nonlabeled $Z_{HER2:342}$. Results are presented as %IA/g.

Scintillation-camera imaging, performed at 1 and 4 h after injection (Fig. 3), confirmed the results of the biodistribution experiments. The tumor xenografts were the only sites with prominent accumulation of radioactivity. The kidneys were visualized at 1 h after injection, but at 4 h after injection only the HER2-expressing tumor xenografts were clearly visible.

Dosimetry

The evaluation of absorbed doses in mice for ^{188}Re-$Z_{HER2:V2}$ is presented in Table 2. The self-doses to most organs and tissues were much smaller than absorbed doses to tumors. However, the size of a mouse body is comparable to the range of the β particles emitted by ^{188}Re (~10 mm). For this reason, the total absorbed doses became much higher because of cross-irradiation. For example, the total absorbed dose to bone marrow was approximately 22% of the total absorbed dose to tumor. Thus, it was impossible to deliver a therapeutically meaningful absorbed dose to tumors (>50 Gy) without delivering a lethal absorbed dose to the red marrow (~8 Gy for mice). Performing experiments with ^{188}Re-$Z_{HER2:V2}$ therapy in mice was thus considered unethical under these circumstances, and because of dimensional differences between mice and humans and the range of β particles, experiments in murine models will generate irrelevant results.

The results of estimated absorbed dose calculations of ^{188}Re-$Z_{HER2:V2}$ in humans using OLINDA/EXM 1.0 are presented in Table 3. In brief, tumor standardized uptake value was approximately constant after 1 h, with a mean value of 3.3. Assuming local deposition of all β energy, and no self- or cross-dose from γ photons, this would result in an absorbed dose to tumor of 0.65 mGy/MBq. As shown in Figure 4, absorbed doses to tumors with a weight of less than 10 g would be slightly lower because of incomplete absorption of β particles, whereas slightly higher absorbed doses are expected in larger tumors due to self-dose from γ radiation. Absorbed dose to tumor exceeded absorbed dose to kidney and bone marrow by 3.4-fold and 79-fold, respectively.

DISCUSSION

Radioimmunotherapy of radiosensitive hematologic malignancies has proven to be successful, but treatment of more radioresistant solid tumors has so far been inefficient. The main reason is a failure to reach tumor-absorbed doses above 50 Gy, which are typically required to achieve a response to external-beam therapy (*7*).

Clinical experience with targeted radionuclide therapy using short peptides, particularly somatostatin analogs, demonstrated

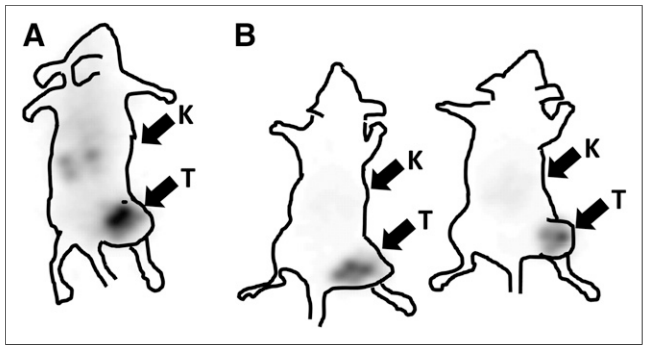

FIGURE 3. Imaging of HER2 expression in SKOV-3 ovarian cancer xenografts (high HER2 expression) in NMRI *nu/nu* mice using ^{188}Re-$Z_{HER2:V2}$. Planar scintillation-camera images were acquired at 1 h (A) and 4 h (B) after injection. Arrows point to tumors (T) and kidneys (K).

TABLE 2
Calculated Absorbed Dose (Gy/MBq) for ^{188}Re-$Z_{HER2:V2}$ in Mice Using Murine Moby Phantom

Organ	Self-dose	Total absorbed dose
Blood	0.008	0.099
Heart	0.003	0.094
Lung	0.019	0.14
Salivary gland	0.0062	0.11
Thyroid	0.00022	0.13
Liver	0.027	0.079
Spleen	0.0068	0.072
Pancreas	0.0024	0.075
Stomach	0.014	0.061
Small intestine	0.0058	0.076
Large intestine	0.0051	0.11
Kidney	0.17	0.23
Skin	0.0038	0.081
Bone	0.0019	0.10
Brain	0.00073	0.026
Carcass	0.16	0.16
Tumor 1	0.40	0.43
Tumor 2	0.40	0.43
Tumor 3	0.40	0.44
Bone marrow	0.0029	0.096

Tumors 1, 2, and 3 stand for tumors in right hind leg, left hind leg, and left flank, respectively.

that the use of small targeting agents can solve the problem of both poor tumor penetration and exposure of bone marrow (*30*). Unfortunately, all small HER2-targeting radiolabeled agents, including antibody fragments, diabodies, designed ankyrin repeat proteins, and Affibody molecules, undergo considerable renal reabsorption (*31*). In the case of residualizing radiometal labels, the renal uptake would be higher than tumor uptake for all these targeting proteins.

Our approach is based on knowledge of the cellular processing of Affibody molecules. The main hypothesis was that the use of a nonresidualizing label would cause rapid clearance from kidneys, where Affibody molecules are rapidly internalized and degraded and their radiocatabolites excreted from cells. At the same time, processing of Affibody molecules bound to HER2-expressing cancer cells is slow, and cellular retention is good even in the case of nonresidualizing labels. Our previous structure–property relationship studies demonstrated that the use of a -GGGC peptide–based chelator yields nonresidualizing ^{99m}Tc labels (*22*) with low accumulation in kidneys. The present study has shown that $Z_{HER2:V2}$ can be efficiently labeled with ^{188}Re. The high-fidelity refolding of Affibody molecules under physiologic conditions (*32*) permitted their direct rhenium labeling at high temperature with high yields. In fact, ^{188}Re-$Z_{HER2:V2}$ preserved high-affinity binding (6.4 ± 0.4 pM) to HER2-expressing cells after labeling at 90°C and pH 4.2. Although an in vitro processing study (Fig. 1) showed low intracellular retention of radiocatabolites, the overall retention of radioactivity was reasonable, with a biologic half-life of 19.6 h. ^{188}Re-$Z_{HER2:V2}$ has shown specific uptake in HER2-expressing xenografts in vivo (Fig. 2). The biodistribution study confirmed that unbound radioactivity cleared quickly from blood, and release of retained radioactivity was much more rapid from kidneys than from tumors (Table 1). The area under the curve for tumor was 47-fold greater than that for blood, 70-fold greater than that for bone, and 2.8-fold greater than that for kidneys. This finding suggests that the goal of delivering an efficient absorbed dose to tumors while sparing critical organs may be achievable.

We performed dosimetry calculations for ^{188}Re-$Z_{HER2:V2}$ in mice using the anatomically realistic murine Moby phantom (*27,28*). The self-doses agreed with area-under-curve data, but the total absorbed dose to bone marrow was much higher than the self-dose. A high total absorbed dose to bone marrow is a phenomenon associated with mice as an animal model. The maximum range of β particles from ^{188}Re is 10.4 mm (*7*), which is comparable to the dimensions of a mouse. For this reason, the cross-dose to bone marrow is much higher in mice than in humans. Delivery of therapeutically meaningful absorbed doses to tumors in mice would be associated with lethal absorbed doses to bone marrow.

Human dosimetry is much different because of the larger dimensions of the human body. Upscaling of murine biodistribution data to

TABLE 3
Calculated Absorbed Dose (mGy/MBq) for ^{188}Re-$Z_{HER2:V2}$ in Humans Using OLINDA/EXM 1.0

Organ	Absorbed dose, ^{188}Re-$Z_{HER2:V2}$
Adrenals	0.007
Brain	0.002
Breasts	0.006
Gallbladder wall	0.007
Lower large intestine wall	0.022 (0.046*)
Small intestine	0.018 (0.014*)
Stomach wall	0.007
Upper large intestine wall	0.034
Heart wall	0.006
Kidneys	0.189
Liver	0.029
Lungs	0.011
Muscle	0.006
Ovaries	0.007
Pancreas	0.006
Red marrow	0.010
Osteogenic cells	0.020
Skin	0.006
Spleen	0.009
Thymus	0.006
Thyroid	0.001
Urinary bladder wall	0.006
Uterus	0.007
Total body	0.009
Tumor	0.65

*Using gastrointestinal tract model assuming 0.35% of injected dose entering small intestine.

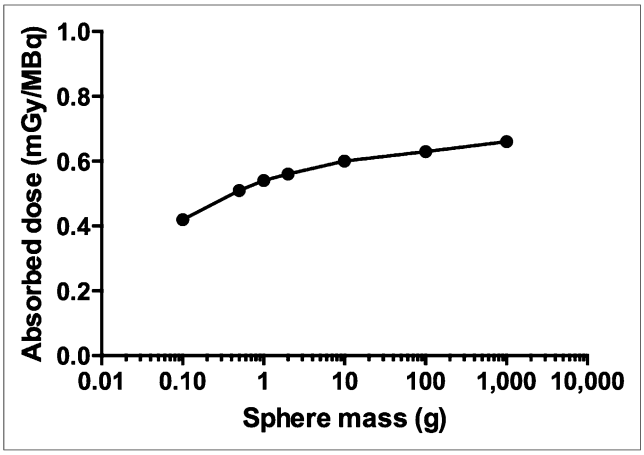

FIGURE 4. Tumor-absorbed dose vs. mass for ^{188}Re-$Z_{HER2:V2}$.

humans suggests that much lower absorbed doses will be delivered to radiosensitive organs in relation to tumor-absorbed doses. A maximum absorbed dose of 2 Gy for bone marrow is generally accepted when radionuclide therapy is being planned, as such an absorbed dose is associated with a low risk that leukemia will develop (*33*) and a low risk for acute bone marrow toxicity. An absorbed dose of 23 Gy is a commonly used limit for kidneys in peptide receptor radionuclide therapy (*34*). In the case of ^{188}Re-$Z_{HER2:V2}$, an absorbed dose of 23 Gy to the kidneys would correspond to a tumor-absorbed dose of 79 Gy, whereas an absorbed dose of 2 Gy to the bone marrow would correspond to a tumor-absorbed dose of 130 Gy. Thus, an absorbed dose of well above 50 Gy could be delivered without exceeding commonly accepted absorbed dose limits to critical organs. However, upscaling from mice to humans is associated with apparent uncertainties, and a clinical imaging study would be required to more reliably assess human dosimetry.

In addition to dosimetry estimations, there are other factors to consider when planning future therapy applications. ^{188}Re is produced via a generator in no-carrier-added form, which provides high specific activity. The short half-life of ^{188}Re enables irradiation of tumors with a high dose rate. Close matching of physical and biologic half-lives and generator-mediated production from the long-lived mother nuclide ^{188}W (half-life, 70 d) permits fractionated therapy. Both the absorbed dose rate during tumor irradiation and treatment fractionation are considered important radiobiologic factors for increasing the efficacy of targeted radionuclide therapy (*7*).

One important lesson from this study concerns the selection of labeling strategy. It is common knowledge that the selection of radionuclide and chelator influences the stability of nuclide attachment to a targeting protein and intracellular retention of radioactivity after internalization. Our earlier studies demonstrated that modification of the physicochemical properties of Affibody molecules by incorporation of a radionuclide–chelator complex also modifies off-target interactions, changing blood clearance rate, the predominant excretion pathway, and biodistribution (*11*). These factors can be used to optimize targeting properties. We demonstrated earlier that the ^{186}Re-maGSG-$Z_{HER2:342}$ Affibody molecule, having an N-terminal mercaptoacetyl-glycyl-seryl-glycyl chelator, shows better retention of radioactivity in tumors than in kidneys (*25*). However, appreciable hepatobiliary excretion of ^{186}Re-maGSG-$Z_{HER2:342}$ (20% of injected radioactivity was measured in the intestinal content at 4 h after injection) caused a risk of high absorbed dose to intestines. Through reengineering of Affibody molecules by modifying the chelator and its placement to the C terminus, as well as by increasing the hydrophilicity of the N terminus by amino acid substitution, we suppressed hepatobiliary excretion of ^{188}Re-$Z_{HER2:V2}$ while keeping good tumor retention, low renal uptake, and rapid clearance of unbound radioactivity. Thus, optimal molecular design, including labeling strategy, may appreciably improve the properties of scaffold-protein–based conjugates for radionuclide therapy.

CONCLUSION

The Affibody molecule $Z_{HER2:V2}$ can be labeled with ^{188}Re with a high yield and preserved picomolar affinity to HER2. ^{188}Re-$Z_{HER2:V2}$ provides efficient targeting of HER2-expressing xenografts, rapid blood clearance, and low uptake in kidneys and bones. Dosimetry calculations in humans suggest that ^{188}Re-$Z_{HER2:V2}$ may provide an absorbed dose to tumors of more than 70 Gy while keeping the absorbed dose to kidneys below 23 Gy and the absorbed dose to bone marrow below 2 Gy. Thus, ^{188}Re-$Z_{HER2:V2}$ is a promising targeting agent for radionuclide therapy against HER2-expressing tumors.

DISCLOSURE

The costs of publication of this article were defrayed in part by the payment of page charges. Therefore, and solely to indicate this fact, this article is hereby marked "advertisement" in accordance with 18 USC section 1734. This research was supported in part by grants from the Swedish Cancer Society (Cancerfonden), Swedish Research Council (Vetenskapsrådet), and Governmental Funding of Clinical Research within the National Health Service (ALF). No other potential conflict of interest relevant to this article was reported.

REFERENCES

1. Slamon DJ, Leyland-Jones B, Shak S, et al. Use of chemotherapy plus a monoclonal antibody against HER2 for metastatic breast cancer that overexpresses HER2. *N Engl J Med.* 2001;344:783–792.
2. Bang YJ, Van Cutsem E, Feyereislova A, et al. Trastuzumab in combination with chemotherapy versus chemotherapy alone for treatment of HER2-positive advanced gastric or gastro-oesophageal junction cancer (ToGA): a phase 3, open-label, randomised controlled trial. *Lancet.* 2010;376:687–697.
3. Wu AM, Senter PD. Arming antibodies: prospects and challenges for immunoconjugates. *Nat Biotechnol.* 2005;23:1137–1146.
4. Diéras V, Bachelot T. The success story of trastuzumab emtansine, a targeted therapy in HER2-positive breast cancer. *Target Oncol.* July 14, 2013 [Epub ahead of print].
5. Sharkey RM, Goldenberg DM. Perspectives on cancer therapy with radiolabeled monoclonal antibodies. *J Nucl Med.* 2005;46(suppl 1):115S–127S.
6. Kenanova V, Wu AM. Tailoring antibodies for radionuclide delivery. *Expert Opin Drug Deliv.* 2006;3:53–70.
7. Pouget JP, Navarro-Teulon I, Bardiès M, et al. Clinical radioimmunotherapy: the role of radiobiology. *Nat Rev Clin Oncol.* 2011;8:720–734.
8. Miao Z, Levi J, Cheng Z. Protein scaffold-based molecular probes for cancer molecular imaging. *Amino Acids.* 2011;41:1037–1047.
9. Nygren PA. Alternative binding proteins: Affibody binding proteins developed from a small three-helix bundle scaffold. *FEBS J.* 2008;275:2668–2676.
10. Orlova A, Magnusson M, Eriksson TL, et al. Tumor imaging using a picomolar affinity HER2 binding Affibody molecule. *Cancer Res.* 2006;66:4339–4348.
11. Feldwisch J, Tolmachev V. Engineering of Affibody molecules for therapy and diagnostics. *Methods Mol Biol.* 2012;899:103–126.
12. Baum RP, Prasad V, Müller D, et al. Molecular imaging of HER2-expressing malignant tumors in breast cancer patients using synthetic ^{111}In- or ^{68}Ga-labeled Affibody molecules. *J Nucl Med.* 2010;51:892–897.
13. Sörensen J, Sandberg D, Sandström M, et al. First-in-human molecular imaging of HER2 expression in breast cancer metastases using the ^{111}In-ABY-025 Affibody molecule. *J Nucl Med.* 2014;55:730–735.

14. Altai M, Varasteh Z, Andersson K, Eek A, Boerman O, Orlova A. In vivo and in vitro studies on renal uptake of radiolabeled Affibody molecules for imaging of HER2 expression in tumors. *Cancer Biother Radiopharm.* 2013;28:187–195.
15. Wållberg H, Orlova A. Slow internalization of anti-HER2 synthetic Affibody monomer ^{111}In-DOTA-ZHER2:342-pep2: implications for development of labeled tracers. *Cancer Biother Radiopharm.* 2008;23:435–442.
16. Tolmachev V, Mume E, Sjöberg S, Frejd FY, Orlova A. Influence of valency and labelling chemistry on in vivo targeting using radioiodinated HER2-binding Affibody molecules. *Eur J Nucl Med Mol Imaging.* 2009;36:692–701.
17. Engfeldt T, Tran T, Orlova A, Widström C, Karlström AE, Tolmachev V. ^{99m}Tc-chelator engineering to improve tumour targeting properties of a HER2-specific Affibody molecule. *Eur J Nucl Med Mol Imaging.* 2007;34:1843–1853.
18. Tran T, Engfeldt T, Orlova A, et al. ^{99m}Tc-maEEE-$Z_{HER2:342}$, an Affibody molecule-based tracer for the detection of HER2 expression in malignant tumors. *Bioconjug Chem.* 2007;18:1956–1964.
19. Tran TA, Ekblad T, Orlova A, et al. Effects of lysine-containing mercaptoacetyl-based chelators on the biodistribution of ^{99m}Tc-labeled anti-HER2 Affibody molecules. *Bioconjug Chem.* 2008;19:2568–2576.
20. Ekblad T, Tran T, Orlova A, et al. Development and preclinical characterisation of ^{99m}Tc-labelled Affibody molecules with reduced renal uptake. *Eur J Nucl Med Mol Imaging.* 2008;35:2245–2255.
21. Ahlgren S, Wållberg H, Tran TA, et al. Targeting of HER2-expressing tumors with a site-specifically ^{99m}Tc-labeled recombinant Affibody molecule, ZHER2:2395, with C-terminally engineered cysteine. *J Nucl Med.* 2009;50:781–789.
22. Wållberg H, Orlova A, Altai M, et al. Molecular design and optimization of ^{99m}Tc-labeled recombinant Affibody molecules improves their biodistribution and imaging properties. *J Nucl Med.* 2011;52:461–469.
23. Altai M, Wållberg H, Orlova A, et al. Order of amino acids in C-terminal cysteine-containing peptide-based chelators influences cellular processing and biodistribution of ^{99m}Tc-labeled recombinant Affibody molecules. *Amino Acids.* 2012;42:1975–1985.
24. Cyr JE, Pearson DA, Wilson DM, et al. Somatostatin receptor-binding peptides suitable for tumor radiotherapy with Re-188 or Re-186: chemistry and initial biological studies. *J Med Chem.* 2007;50:1354–1364.
25. Orlova A, Tran TA, Ekblad T, Karlström AE, Tolmachev V. ^{186}Re-maGSG-Z (HER2:342), a potential Affibody conjugate for systemic therapy of HER2-expressing tumours. *Eur J Nucl Med Mol Imaging.* 2010;37:260–269.
26. Wållberg H, Löfdal PÅ, Tschapalda K. Affinity recovery of eight HER2-binding Affibody variants using an anti-idiotypic Affibody molecule as capture ligand. *Protein Expr Purif.* 2011;76:127–135.
27. Larsson E, Strand SE, Ljungberg M, Jönsson BA. Mouse S-factors based on Monte Carlo simulations in the anatomical realistic Moby phantom for internal dosimetry. *Cancer Biother Radiopharm.* 2007;22:438–442.
28. Larsson E, Ljungberg M, Strand SE, Jönsson BA. Monte Carlo calculations of absorbed doses in tumours using a modified MOBY mouse phantom for pre-clinical dosimetry studies. *Acta Oncol.* 2011;50:973–980.
29. Stabin MG. *Fundamentals of Nuclear Medicine Dosimetry.* New York, NY: Springer; 2008:83–86.
30. van Essen M, Krenning EP, Kam BL, de Jong M, Valkema R, Kwekkeboom DJ. Peptide-receptor radionuclide therapy for endocrine tumors. *Nat Rev Endocrinol.* 2009;5:382–393.
31. Tolmachev V. Imaging of HER-2 overexpression in tumors for guiding therapy. *Curr Pharm Des.* 2008;14:2999–3019.
32. Arora P, Oas TG, Myers JK. Fast and faster: a designed variant of the B domain of protein A folds in 3 microsec. *Protein Sci.* 2004;13:847–853.
33. Forrer F, Krenning EP, Kooij PP, et al. Bone marrow dosimetry in peptide receptor radionuclide therapy with [^{177}Lu-DOTA^{0},Tyr^{3}]octreotate. *Eur J Nucl Med Mol Imaging.* 2009;36:1138–1146.
34. Kwekkeboom DJ, de Herder WW, van Eijck CH, et al. Peptide receptor radionuclide therapy in patients with gastroenteropancreatic neuroendocrine tumors. *Semin Nucl Med.* 2010;40:78–88.